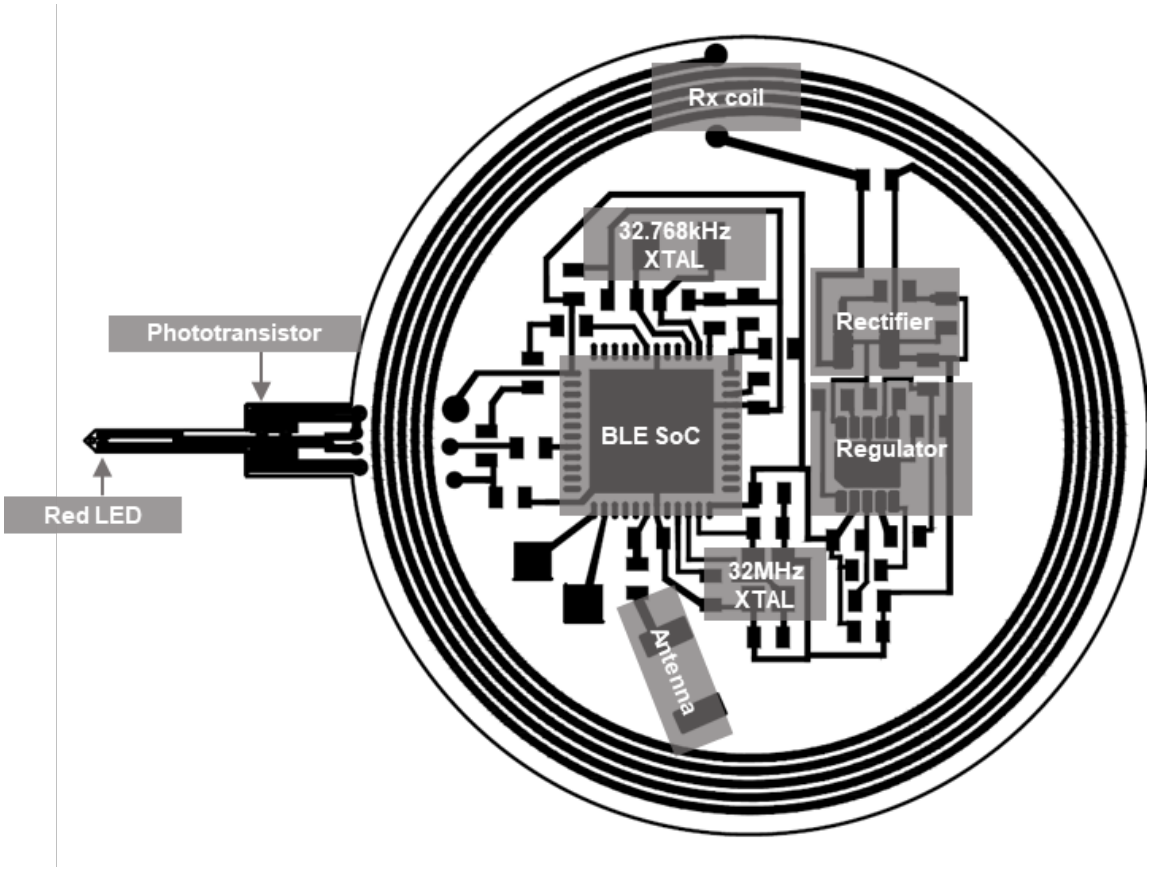

Supplementary Figure 1. Circuit design of wireless PDT device.

Supplementary Table 1. List of circuit components

Name	Part Number / Value	Description
U1	nRF52832-QAAB-R	BLE SoC
U2	BAS40XY	Schottky rectifier
U3	LTC3255HDD	3.3V voltage regulator
I1	APG0603SEC-E-TT	624nm LED
I2	KDT00030	Phototransistor
X1	CX2016DB32000D0WZRC1	32MHz XTAL
X2	ABS07-32.768KHZ-9-T	32.768kHz XTAL
A1	ALA321C3	2.4GHz antenna
R1	40.2kΩ	SMD resistor
R2	220kΩ	SMD resistor
R3	68kΩ	SMD resistor
R4	30kΩ	SMD resistor
R5	29.1Ω	SMD resistor
C1	110pF	SMD capacitor
C2, C4, C9	1uF	SMD capacitor
C3, C8_1, C8_2, C8_3	100nF	SMD capacitor
C5	10uF	SMD capacitor
C6	0.8pF	SMD capacitor
C7_1, C7_2, C7_3, C7_4	12pF	SMD capacitor
C10	4.7uF	SMD capacitor
C11	100pF	SMD capacitor
L1	3.9nH	SMD inductor

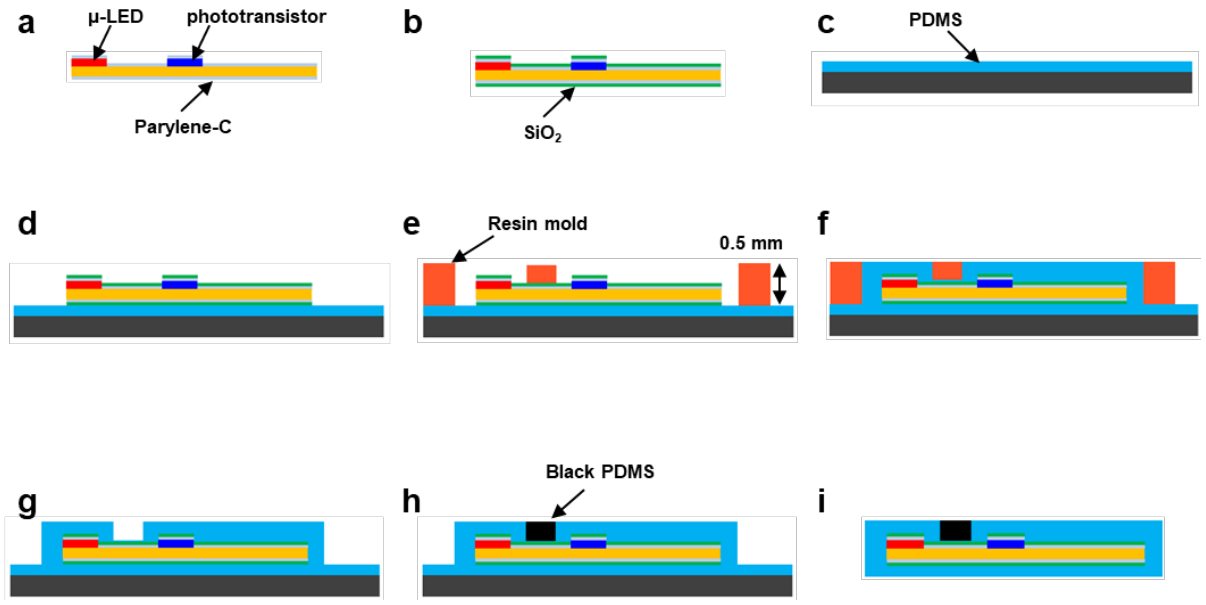

Supplementary Figure 2. Encapsulation process for long-term in vivo operation of the device. a, Depositing Parylene-C around device by parylene coating system; **b**, Depositing SiO2 on the top and bottom of the device by sputter; **c**, Spin coating PDMS on hydrophobic surface-treated Si wafer; **d**, Oxide bonding with device and PDMS; **e**, Placing the resin mold; **f**, Pouring PDMS and curing in vacuum; **g**, Removing resin mold from substrate; **h**, Filling black PDMS between μ-led and phototransistor; **i**, Delaminating the device from the wafer

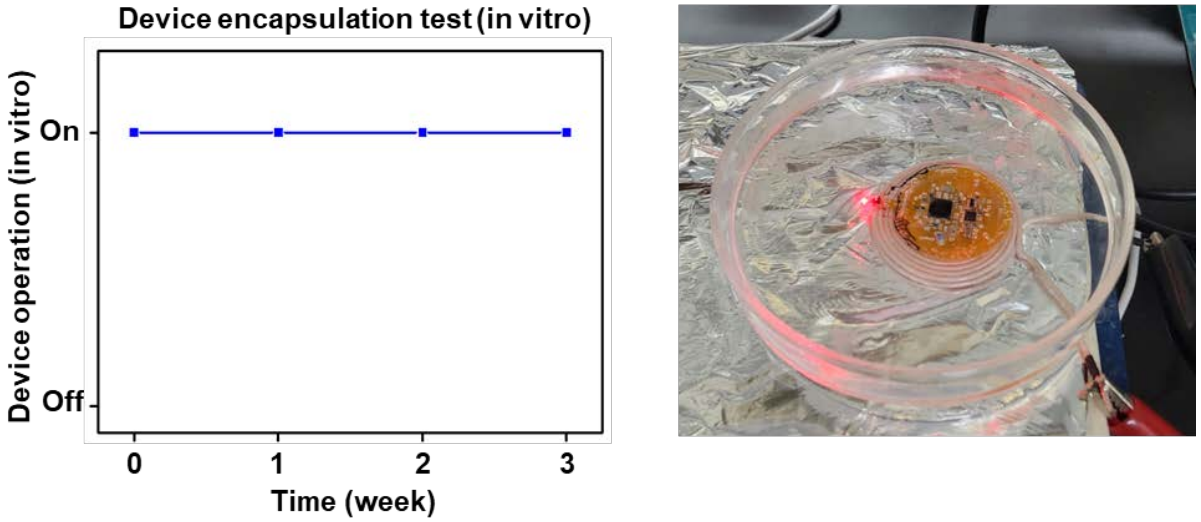

Supplementary Figure 3. ***In vitro*** **device encapsulation test.** The devices (n=5) were confirmed to operate normally over 3 weeks in PBS solution at 37ºC.

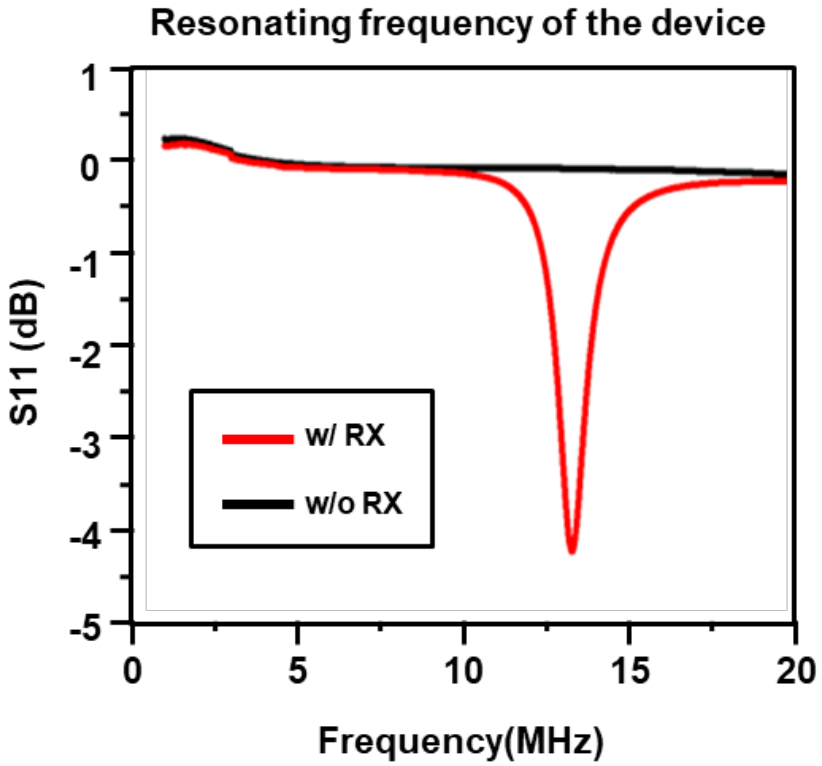

Supplementary Figure 4. S11 parameter measurements on the transmitter coil with and without the device present.

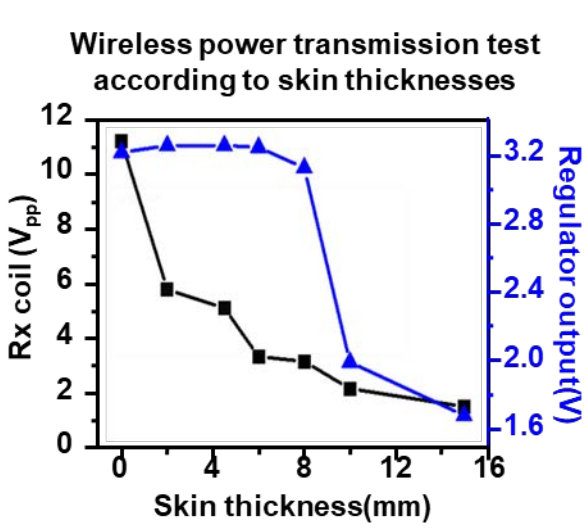

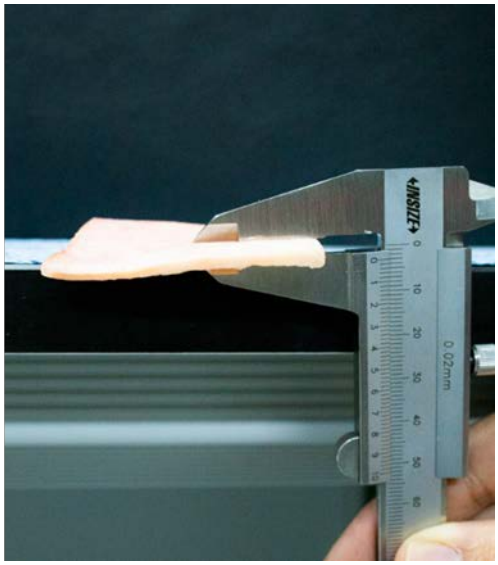

Supplementary Figure 5. The result of measuring the wireless power receiving ability of the device for each skin thickness using pig skin. The skin tissues were placed between the device and the transmitting coil, and the thickness was changed by changing the number of layers of the skin tissues.

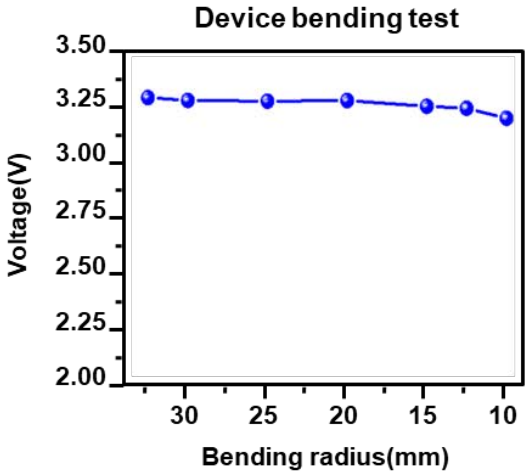

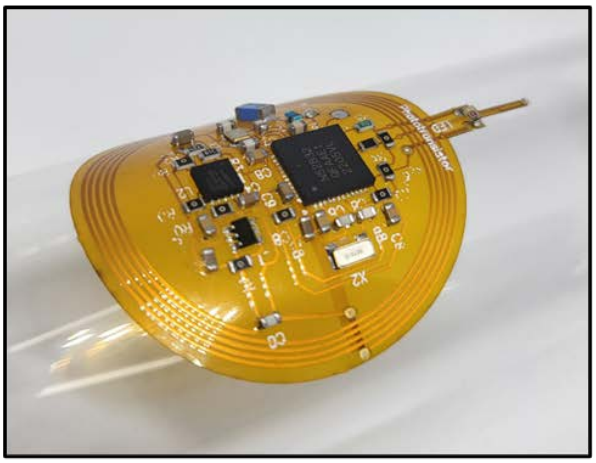

Supplementary Figure 6. Bending test result measuring the change in the supply voltage of the device according to the bending radius from 35mm to 10mm.

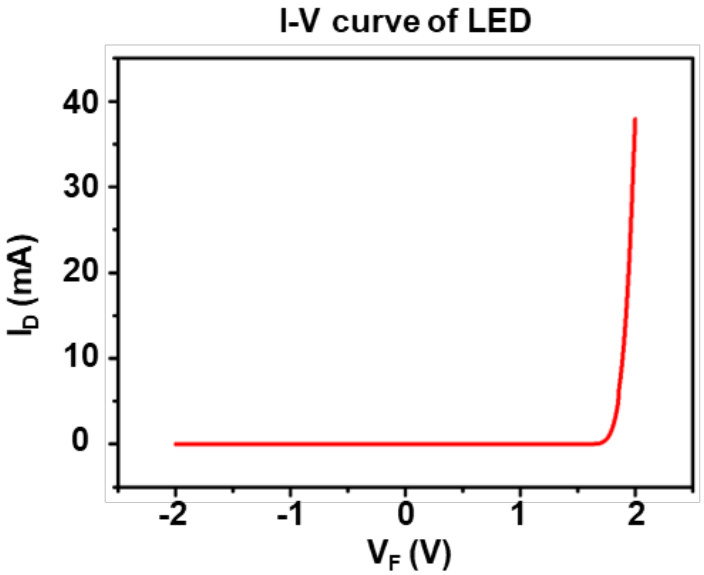

Supplementary Figure 7. I-V characteristic graph of μ-LED used in device

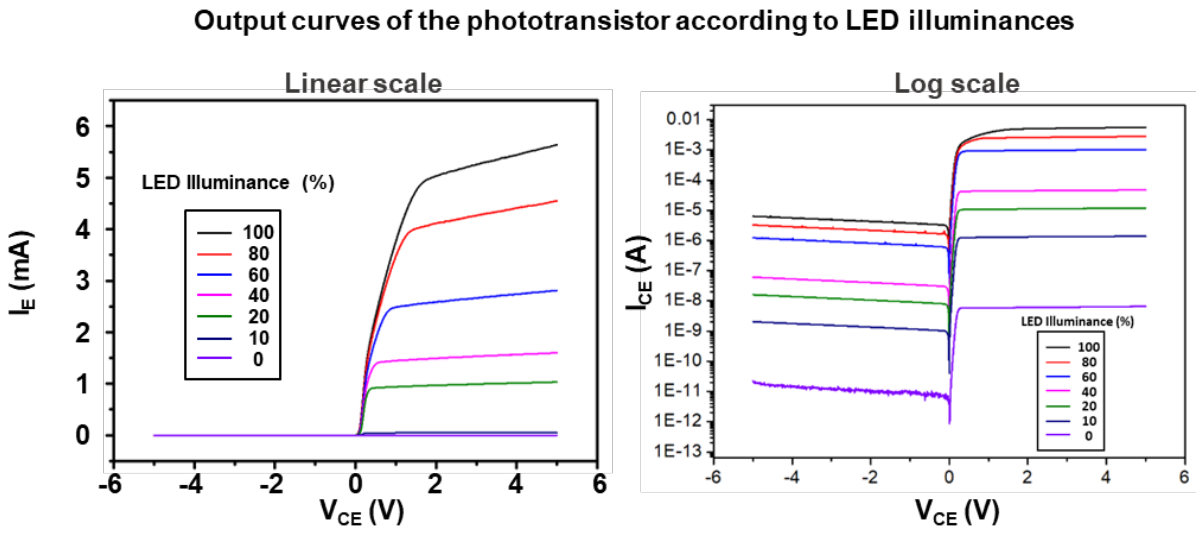

Supplementary Figure 8. Output curves of phototransistor used for optical measurements under different brightness conditions, linear scale (left) and log scale (right).

Supplementary Note 1. Biocompatibility of the device

In order to exclude the risk of biotoxicity that may occur in the process of combining these biocompatible materials, the device was subcutaneously implanted in rats to investigate biocompatibility and inflammatory response (Supplementary Fig.9). Acute and chronic inflammatory responses by the device were evaluated by histological analysis of tissue surrounding the device after 5 days and 2 weeks, respectively. Supplementary Figure 9a shows hematoxylin and eosin (H&E) and Masson's trichrome (MT) images of tissue surrounding the explanted device on day 5 and day 14. In the H&E staining images, the asterisk marks on day 5 indicate the distribution of immune cells including neutrophils, lymphocytes, and macrophages by acute inflammation. The acute inflammatory reaction is expected to be caused by the surgical procedure for device implantation. It is known that acute inflammatory responses caused by external stimuli such as surgery play an important role in supplying growth factor, and cytokine signals necessary for repair process. However, if chronic inflammation is induced by stimuli such as absence of initial treatment, persistent infections, autoimmune reactions, allergic responses, and chemical insults, fibrosis may occur and reduce device sensitivity. As shown in the MT staining image, fibrosis, in which extracellular matrix components including collagen (blue) were excessively deposited, was not observed even after 14 days in the tissue surrounding the implanted device. Furthermore, to evaluate the inflammatory response in more depth, immunofluorescence staining was performed on macrophages that play an important role in the inflammatory response (Supplementary Fig.9b). The cluster of differentiation 68 (CD 68)-positive cells, a pan-macrophage marker, were observed to be distributed in a wide area around the device on day 5, but decreased to 50.90% of day 5 on day 14 (Supplementary Fig.9c). In particular, it was confirmed that the ratio of M2 macrophages, which contribute to tissue healing by producing anti-inflammatory cytokines, to the total macrophages increased 1.85 times on day 14 compared to day 5. These results indicate that the material of the implanted device did not offer chemical and physical stimuli that can induce chronic inflammation. Indeed, in an *in vitro* cytotoxicity assay using the device material extract described in ISO 10993-5:2009, the cell viability of the device material extract was 96.13%, which was similar to the negative control known to be non-toxic (Supplementary Fig.9d). Based on these results, we considered that the device can be used as a biocompatible material in the body without side effects caused by by-products.

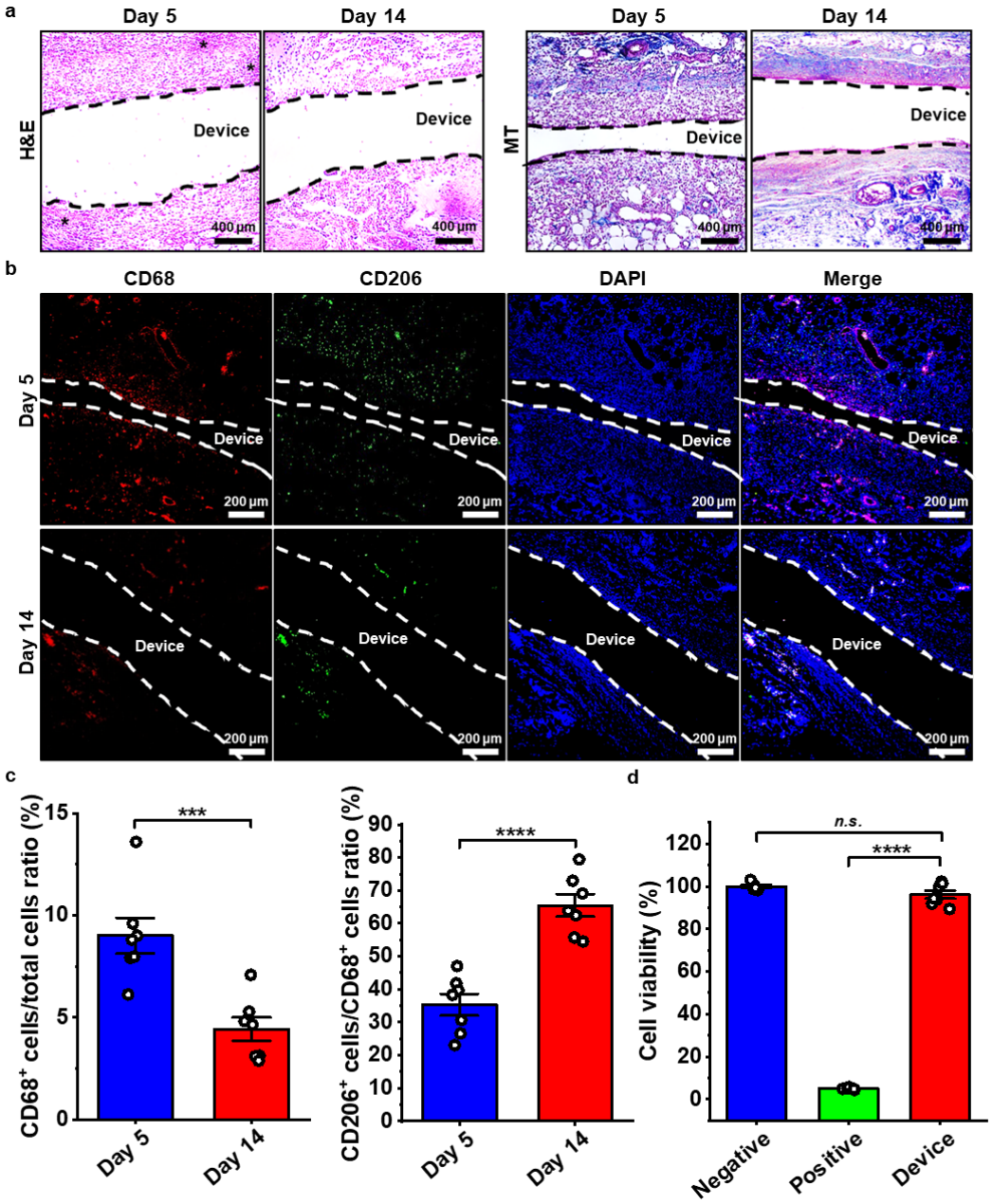

Supplementary Figure 9. ***In vivo*** **and** ***in vitro*** **evaluations on biocompatibility of device. a,** Representative histological images of hematoxylin and eosin (H&E) and Masson's trichrome staining in tissues surrounding the implanted sites at days 5 and 14 after subcutaneous implantations of the device. Black dashed lines indicate the device region, and asterisks indicate inflammatory cells region. **b,** Representative immunofluorescence staining images of macrophages (CD68) and M2 macrophages (CD206) in tissues surrounding the implanted sites at days 5 and 14 after subcutaneous implantations of the device. White dashed lines indicate the device region. **c**, Quantification of CD 68-positive cells to total cell ratios (%), and CD 206-positive cells to CD 68-positive cell ratios (%) to estimate the immune response by macrophages in the tissues surrounding the implanted sites of the device. **d,** *In vitro* cytotoxicity analysis in 50% extracts of materials according to ISO standards. Data are expressed as the mean ± SEM. ***$p < 0.001$, or ****$p < 0.0001$. n.s. = not-significantly different.

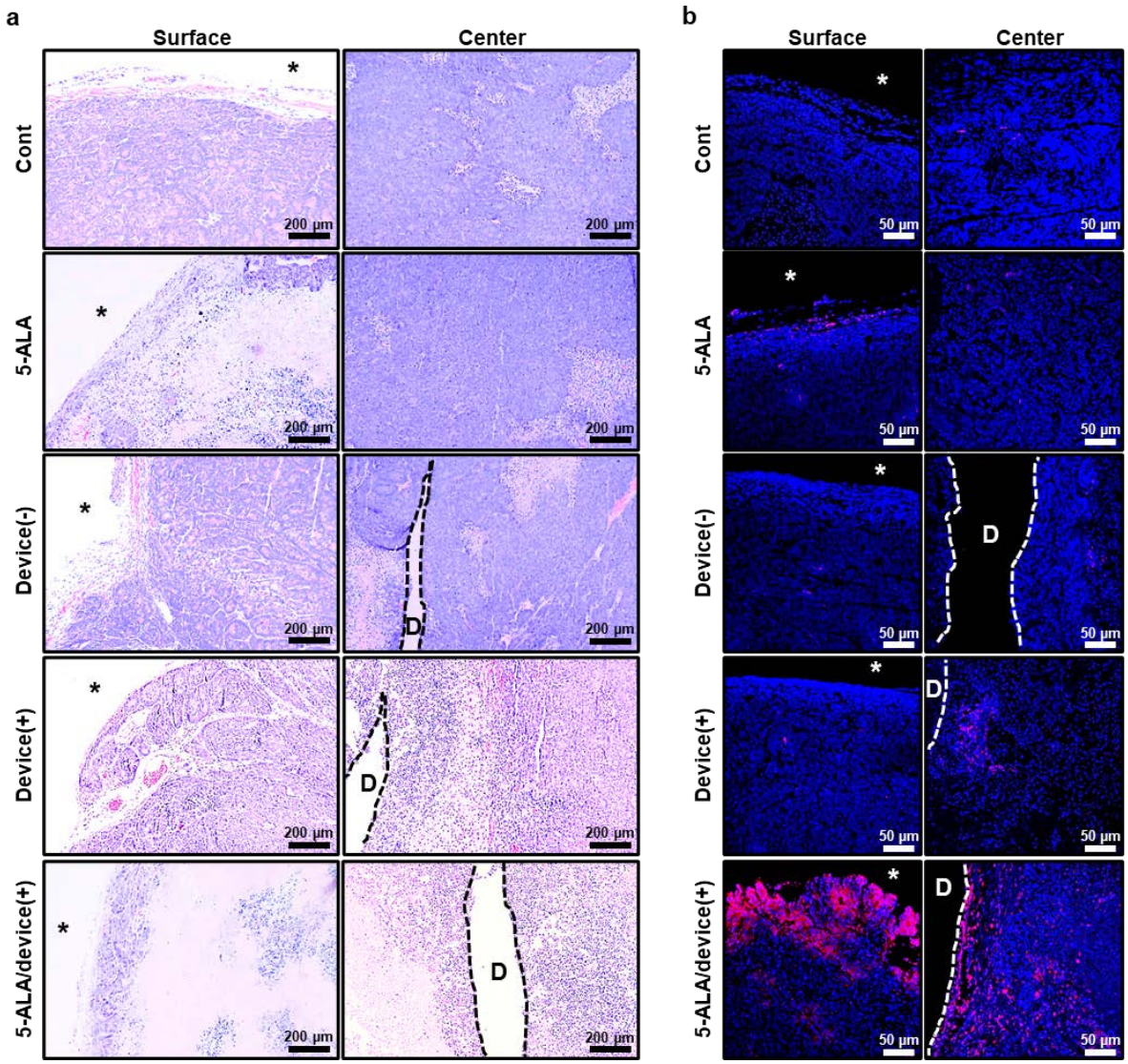

Supplementary Figure 10. Photodynamic therapy efficacy of device on the surface and center of tumor. a, Representative histological images of H&E staining from the surface and center of the excised xenograft tumors 3 weeks after first treatment. Asterisks indicate outside of the excised xenograft tumors, and black dashed lines indicate the device region. **b**, Representative immunofluorescence staining images for apoptosis (caspase 3) from the surface and center of the excised xenograft tumors 3 weeks after first treatment. Asterisks indicate outside of the excised xenograft tumors, and white dashed lines indicate the device region.

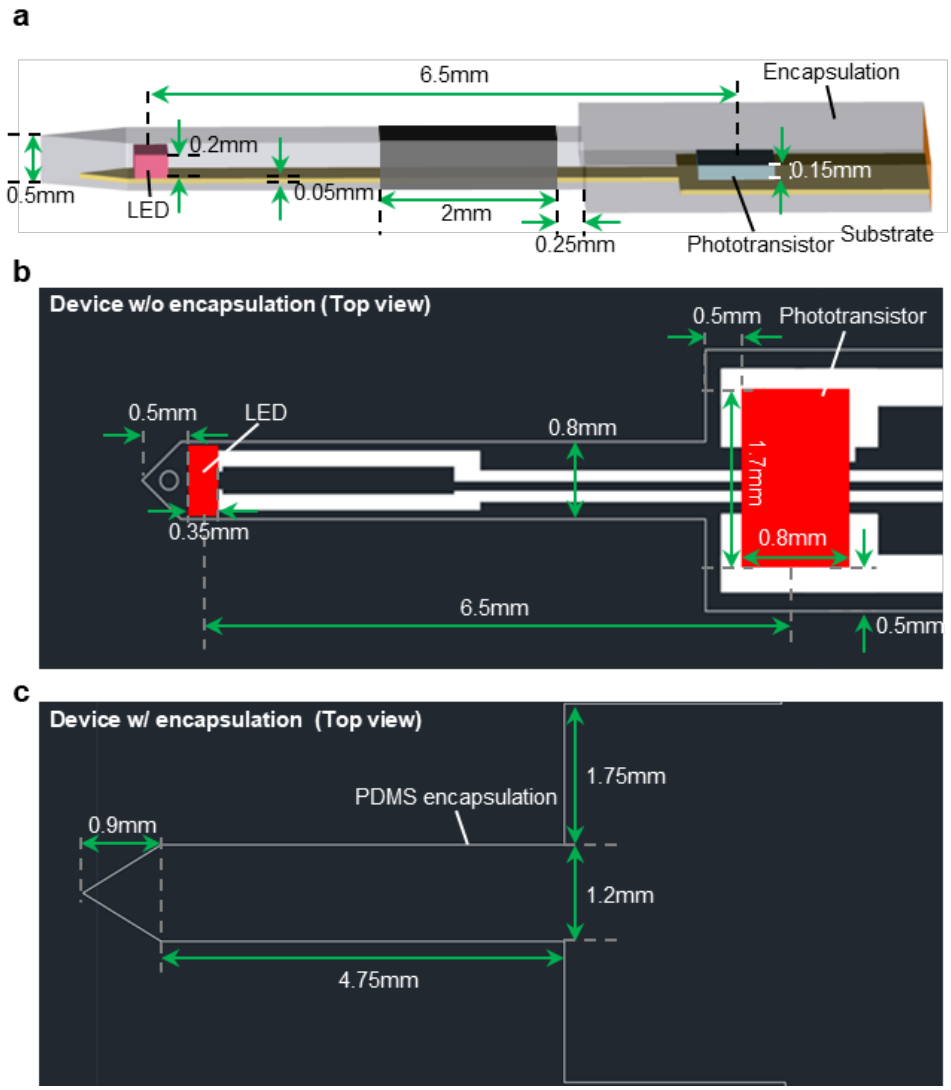

Supplementary Figure 11. Geometrical parameters in the device. (a) Illustration of the cross view of the device. The top view of the device representing the dimensions for (b) the device without encapsulation and (c) with the encapsulation.

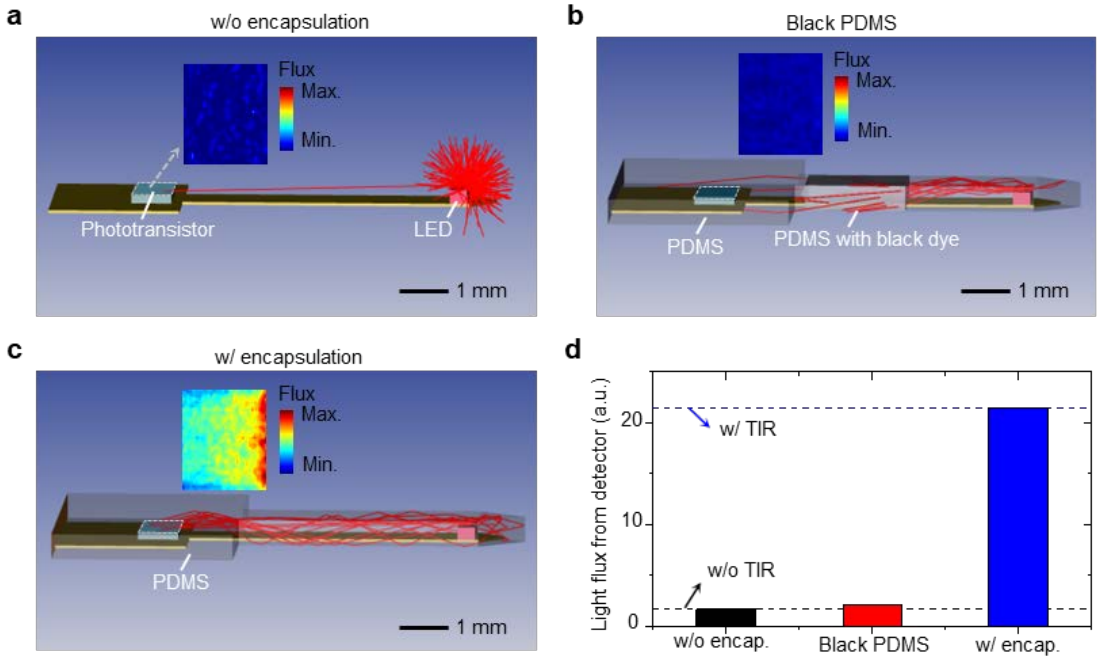

Supplementary Figure 12. Optical effect of encapsulation layer. Scheme of ray-tracing simulation results: (a) without encapsulation, (b) with black PDMS encapsulation, and (c) with PDMS encapsulation. (d) Calculated total light intensity at the phototransistor for w/o encap, black PDMS, and w/ encap.

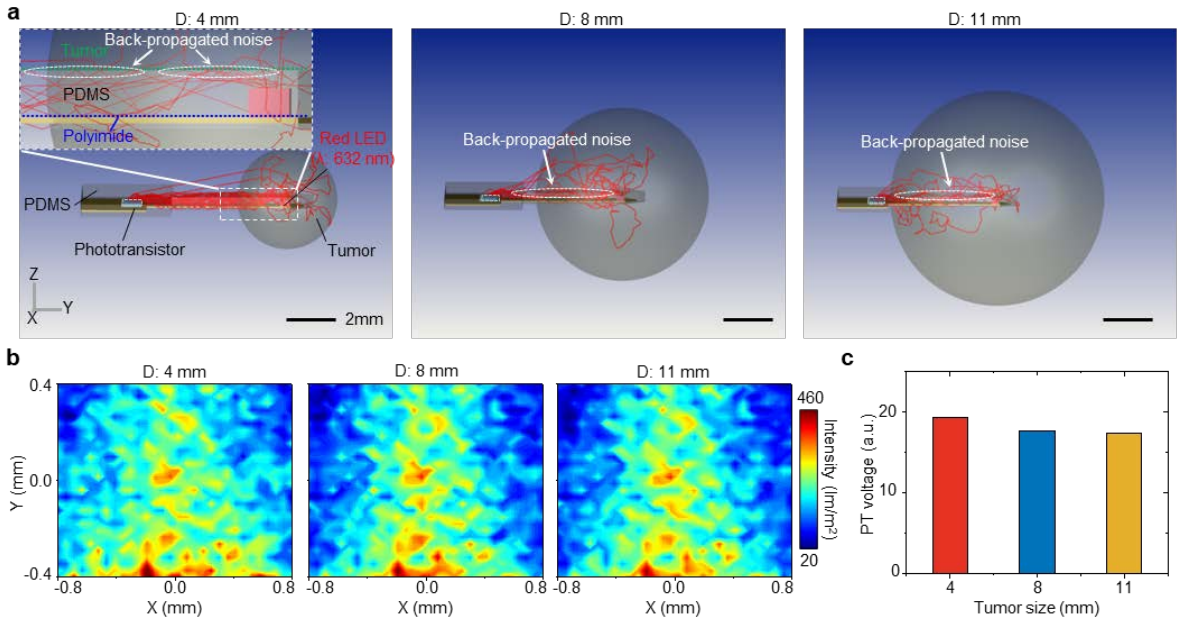

Supplementary Figure 13. Light flux in the PDMS encapsulated device with tumor volume variation. (a) Scheme of ray-tracing simulation result with PDMS encapsulated device as a function of tumor diameter (4 mm; left, 8 mm; middle, and 11 mm; right). (b) Light distribution at phototransistor with three different tumor diameter (4 mm, 8 mm, and 11 mm). (c) The calculated voltage from phototransistor with different tumor size.

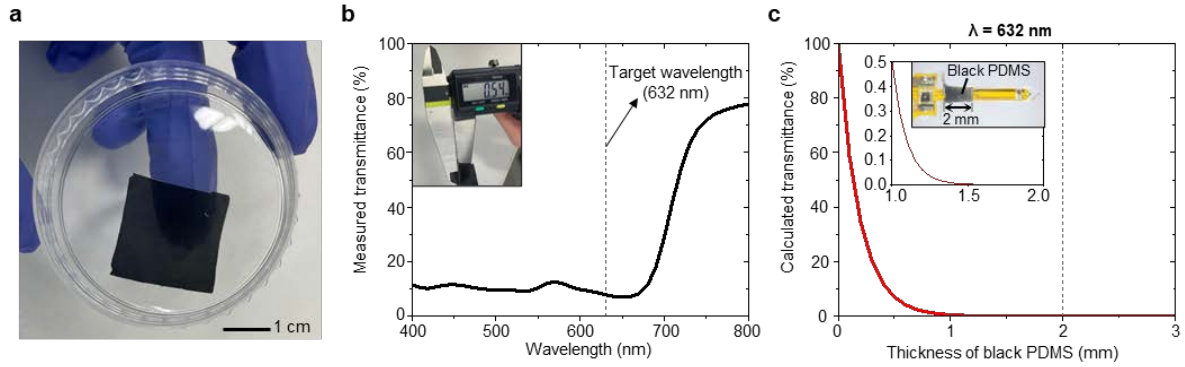

Supplementary Figure 14. Optical characteristic of black PDMS. (a) Optical image of black PDMS. (b) Measured transmittance of black PDMS. Inset image shows the thickness of black PDMS (0.54 mm). (c) Calculated transmittance at 630 nm with different thickness of black PDMS.

Supplementary Table 2. Information for the parameters of the human colon tumor. Optical coefficients of the human colon tumor used in the optical simulations.

Human colon tumor	
Wavelength	632 nm
g	0.868
μ_s (cm^{-1})	120
μ_a(cm^{-1})	1.2
Refractive index	1.348